Zoledronic acid promotes osteoclasts ferroptosis by inhibiting FBXO9-mediated p53 ubiquitination and degradation

Xingzhou Qu [1], Zhaoqi Sun [1], Yang Wang [Coresp., 1], shan Ong Hui [Coresp., 1]

[1] Department of Oral and Maxillofacial-Head & Neck Oncology,, Ninth People's Hospital Affiliated to Shanghai Jiao Tong University School of Medicine, SH, Shanghai, China

Corresponding Authors: Yang Wang, shan Ong Hui
Email address: 115078@sh9hospital.org.cn, 117069@sh9hospital.org.cn

Bisphosphonates (BPs)-related osteonecrosis of jaw (BRONJ) is a severe complication of the long-term administration of BPs. The development of BRONJ is associated with the cell death of osteoclasts, but the underlying mechanism remains unclear. In the current study, the role of Zoledronic acid (ZA), a kind of bisphosphonates, in suppressing the growth of osteoclasts was investigated and its underlying mechanism was explored. The role of ZA in regulating osteoclasts function was evaluated in the RANKL-induced cell model. Cell viability was assessed by cell counting kit-8 (CCK-8) assay and fluorescein diacetate (FDA)-staining. We confirmed that ZA treatment suppressed cell viability of osteoclasts. Furthermore, ZA treatment led to osteoclasts death by facilitating osteoclasts ferroptosis, as evidenced by increased Fe^{2+}, ROS, and malonyldialdehyde (MDA) level, and decreased glutathione peroxidase 4 (GPX4) and glutathione (GSH) level. Next, the gene expression profiles of alendronate- and risedronate-treated osteoclasts were obtained from Gene Expression Omnibus (GEO) dataset, and 18 differentially expressed genes were identified using venn diagram analysis. Among these 18 genes, the expression of F-box protein 9 (FBXO9) was inhibited by ZA treatment. Knockdown of FBXO9 resulted in osteoclasts ferroptosis. More important, FBXO9 overexpression repressed the effect of ZA on regulating osteoclasts ferroptosis. Mechanistically, FBXO9 interacted with p53 and decreased the protein stability of p53. Collectively, our study showed that ZA induced osteoclast cells ferroptosis by triggering FBXO9-mediated p53 ubiquitination and degradation.

1 **Zoledronic acid promotes osteoclasts ferroptosis by inhibiting FBXO9-**

2 **mediated p53 ubiquitination and degradation**

3 Xingzhou Qu, Zhaoqi Sun, Yang Wang*, Hui shan Ong*

4 Department of Oral and Maxillofacial-Head & Neck Oncology, Ninth People's Hospital Affiliated

5 to Shanghai Jiao Tong University School of Medicine, Shanghai 200011, China

6 ***Correspondence author: Hui shan Ong,** Department of Oral and Maxillofacial-Head & Neck

7 Oncology, Ninth People's Hospital Affiliated to Shanghai Jiao Tong University School of

8 Medicine, No. 639, Zhizaoju Road, Shanghai 200011, China. Tel: 86-21-23271699-5160. Email:

9 117069@sh9hospital.org.cn **Yang Wang,** Department of Oral and Maxillofacial-Head & Neck

10 Oncology, Ninth People's Hospital Affiliated to Shanghai Jiao Tong University School of

11 Medicine, No. 639, Zhizaoju Road, Shanghai 200011, China. Tel: 86-21-23271699-5160. Email:

12 Email: 115078@sh9hospital.org.cn

23 **Abstract**

24 Bisphosphonates (BPs)-related osteonecrosis of jaw (BRONJ) is a severe complication of the long-

25 term administration of BPs. The development of BRONJ is associated with the cell death of

26 osteoclasts, but the underlying mechanism remains unclear. In the current study, the role of

27 Zoledronic acid (ZA), a kind of bisphosphonates, in suppressing the growth of osteoclasts was

28 investigated and its underlying mechanism was explored. The role of ZA in regulating osteoclasts

29 function was evaluated in the RANKL-induced cell model. Cell viability was assessed by cell

30 counting kit-8 (CCK-8) assay and fluorescein diacetate (FDA)-staining. We confirmed that ZA

31 treatment suppressed cell viability of osteoclasts. Furthermore, ZA treatment led to osteoclasts

32 death by facilitating osteoclasts ferroptosis, as evidenced by increased Fe^{2+}, ROS, and

33 malonyldialdehyde (MDA) level, and decreased glutathione peroxidase 4 (GPX4) and glutathione

34 (GSH) level. Next, the gene expression profiles of alendronate- and risedronate-treated osteoclasts

35 were obtained from Gene Expression Omnibus (GEO) dataset, and 18 differentially expressed

36 genes were identified using venn diagram analysis. Among these 18 genes, the expression of F-

37 box protein 9 (FBXO9) was inhibited by ZA treatment. Knockdown of FBXO9 resulted in

38 osteoclasts ferroptosis. More important, FBXO9 overexpression repressed the effect of ZA on

39 regulating osteoclasts ferroptosis. Mechanistically, FBXO9 interacted with p53 and decreased the

40 protein stability of p53. Collectively, our study showed that ZA induced osteoclast cells ferroptosis

41 by triggering FBXO9-mediated p53 ubiquitination and degradation.

42 **Keywords:** Bisphosphonates related osteonecrosis of jaw; Zoledronic acid; ferroptosis; FBXO9;

43   p53

44   **Introduction**

45   Bisphosphonates (BPs) inhibit osteoclast activity and disrupt osteoclast mediated bone resorption

46   [1, 2]. BPs are widely used in the treatment of bone metastasis cancer[3], osteoporosis[4], and

47   multiple myeloma[5]. BRONJ is an injury of the jaw that affects patients treated with BPs. Since

48   it was reported in 2003, BRONJ has been considered as a common and important adverse side

49   effect of BPs treatment, especially nitrogen-containing bisphosphonates (Residronate,

50   Alendronate, and Zoledronic acid(ZA))[6]. There are various hypotheses for the development of

51   BRONJ, the most recognized hypothesis was bone remodeling suppression. Although significant

52   progress has been made in prevention and treatment of BRONJ base on the hypotheses, the

53   mechanisms underlying the development of BRONJ remain unclear.

54   Osteoclasts, members of the monocyte/macrophage hematopoietic, play an important role in

55   the progression of bone remodeling[8]. RAW264.7 cells and bone marrow-derived macrophages

56   (BMDMs) can be induced into osteoclasts by receptor activator of nuclear factor-κB ligand

57   (RANKL), and has been widely used as a cell model for the study of osteoclast related diseases *in*

58   *vitro*[9]. The number and the resorptive function of osteoclasts were usually increased during the

59   process of bone remodeling [10]. Therefore, osteoclast is one of the core targets for the treatment

60   of osteoporosis and other bone-remodeling-related diseases. It is well known that ZA can lead to

61   a stronger inhibition of osteoclasts differentiation and induces the apoptosis of osteoclasts[11],

62   while the underlying mechanism of ZA in the function of osteoclasts reminds unclear.

63   Ferroptosis is a recently identified type of iron-mediated cell death. Unlike other forms of

64 programmed cell death, such as apoptosis and necroptosis, ferroptosis does not involve the

65 activation of caspase protein[12, 13]. It is characterized by an increased level of lipid peroxidation

66 products and reactive oxygen species (ROS). The dysregulation of ferroptosis has been related to

67 many pathological processes, such as cancer[14], neurodegenerative diseases[15], and

68 inflammation-related diseases[16]. More and more studies showed that ferroptosis contribute to

69 the development of BRONJ. Jose *et al.* found that the levels of MDA, GSSG, and 8-oxo-dG and

70 the GSSG/GSH ratio in serum and saliva were significantly higher in patients with BRONJ

71 compared with controls[17]. Ma *et al*. demonstrated that melatonin suppresses osteoblast

72 ferroptosis and improved the osteogenic capacity of MC3T3-E1 by activating the Nrf2/HO-1

73 pathway[18]. However, whether ferroptosis was involved in the osteoclasts differentiation and

74 death induced by ZA is still unknown. In the current study, we showed that ZA inhibits the

75 osteoclasts viability in a dose-dependent manner. For the first time, we showed that ZA promotes

76 the ferroptosis of osteoclast by increasing the protein stability of p53. ZA-induced downregulation

77 of ubiquitin E3 ligase FBXO9, and FBXO9 overexpression restores cell viability inhibition of

78 osteoclast induced by ZA. Moreover, FBXO9 facilitates ubiquitination-mediated degradation of

79 p53.

80

81 **Materials and methods**

82 **Cell culture**

83   RAW264.7 cells were purchased from the ATCC (TIB-71, Manassas, VA, USA) and cultured in

84 alpha-Modified Eagle's Medium (α-MEM, Gibco, USA) with 100 U/ml penicillin, and 100 μg/ml

85   streptomycin at 37 °C in a humidified atmosphere containing 5% CO_2 and 95% air. To BMDMs,

86   bone marrow cells were purchased from the ATCC (CRL-2420, Manassas, VA, USA) and cultured

87   in RPMI 1640 medium (Thermo Fisher Scientific, Waltham, MA, USA) for 6 days with 100 U/ml

88   penicillin, 100 μg/ml streptomycin, 10% FBS, and 10 ng/mL recombinant mouse macrophage

89   colony-stimulating factor (PeproTech). For osteoclast formation assay.RAW264.7 cells were

90   seeded in 12-well plate s ($1×10^4$ cells/well) supplemented with 50 ng/ml RANKL (R&D Systems.)

91   for 6 days. BMDMs ($1×10^4$ cells/well) were cultured in the presence of M-CSF (10 ng/mL) and

92   RANKL (50 ng/mL) for 6 days.

93   **TRAP staining**

94   TRAP histochemical staining was performed to confirm the osteoclast as previously described[25],

95   by using an acid phosphatase, leukocyte (TRAP) kit (Sigma-Aldrich). Brifely, $1×10^5$ BMDMs or

96   RAW264.7 induced osteoclasts were then fixed in 10% neutral-buffered formalin (NBF) solution

97   for 20 minutes, then the NBF solution was replaced with TRAP staining solution and 0.1% Fast

98   Red AS TR salt at RT. After 45 minutes cells were washed with $1×$ PBS for three times and

99   imaged.

100   **Measurement of cell viability**

101   Cell viability of BMDMs and RAW264.7 was assessed by using a CCK-8 and FDA assay

102   (Dojindo, Japan). For CCK-8 assay, BMDMs and RAW264.7 cells ($1×10^4$ cells per well) were

103   seeded in 96-well plates for 24 hours, then cells were treated with different doses of ZA (5, 10,

104   and 50μM) for 48 h. To analyze the cells death of osteoclast, BMDMs, and RAW264.7 ($5×10^3$

105   cells per well) were treated with 10μM of ZVAD-FMK, 2μM of Fer-1, or 10μM of necrostatin-1,

106   for 48 h with or without ZA (50μM). Then, a total 10μL of CCK-8 reagent was added to each well

107   additional 4 h at 37°C with 5% CO_2, and the absorbance at 450 nm of each well was assayed using

108   a microplate reader (BioTek Instruments). For FDA assay, **a**fter culture with different dose ZA (5,

109   10, and 50μM) for 48h, BMDMs and RAW264.7 cells were treated with 10μl of FDA solution (5

110   mg/mL; Invitrogen, CA, USA) at 37°C with 5% CO_2 for 20 minutes, then cells images were

111   obtained using a fluorescence microscope (Olympus Corporation, Japan).

112   **Fe^{2+} concentration**

113   The concentration of Ferrous iron (Fe^{2+}) in BMDMs and RAW264.7 cells in the presence or

114   absence of ZA (50μM) was assessed using an iron assay kit (MAK025, Sigma-Aldrich, MO, USA)

115   as the manufacturer's instructions. Briefly, cell samples were incubated with 10 μL of iron reducer

116   for 30 minutes at RT, then 100 μL iron probe was added to trigger the reaction; thus, the absorbance

117   was measured at 593 nm.

118   **Lipid reactive oxygen species (ROS) assay**

119   Lipid ROS level in BMDMs and RAW264.7 cells in the presence or absence of ZA (50μM) was

120   assayed using C11-BODIPY (Invitrogen), a fluorescent-labelled oxidation sensitive probe. In

121   brief, BMDMs and RAW264.7 cells were seeded in 24-well plates ($5×10^5$/well) and treated with

122   ZA (50μM) with or without FBXO9 overexpression for 48h, then BMDMs and RAW264.7 cells

123   were cultured with C11-BODIPY probe with a final concentration of 1μM in at 37°C with 5% CO_2

124   for 30 minutes, then the Lipid ROS levels were assayed using flow cytometer.

125   **MDA and GSH content**

126   MDA in BMDMs and RAW264.7 cells was analyzed using a lipid peroxidation assay kit

127 (ab118970, Abcam) in the presence or absence of ZA (50μM). GSH content in BMDMs and

128 RAW264.7 cells was assayed using a Glutathione Assay Kit (ab65322, Abcam) according to the

129 standard protocol. Briefly, cell supernatant, 5,5′-dithio-bis 2-nitrobenzoic acid solution and the

130 reagents of kits were mixed together and incubated at RT for 10 minutes, then NADPH was added

131 into this system to trigger the reaction. the absorbance of 5-thio-2-nitrobenzoic acid was detected

132 at 412 nm.

133 **Transient transfection of FBXO9 or si-FBXO9**

134 The recombinant plasmids pcDNA-FBXO9 containing FBXO9 cDNA were sub-cloned into

135 pcDNA3.1 vector via EcoR V/Hind III sites. To overexpress FBXO9, the pcDNA-FBXO9 was

136 transfected into BMDMs cells using Lipofectamine 2000. FBXO9 Knockdown and

137 transfection were performed according to the manufacturer's instructions. Briefly, cells were

138 transfected with 10 nM of si-FBXO9 RNA (sense AUCAGAAUGACAAUCUUCCUCU,

139 antisense GGAAGAUUGUCAUUCUGAUGCU

140) or si-Control RNA (sense CAGUCGCGUUUGCGACUGGUU, antisense CCAGUCG-

141 CAAACGCGACUGUU), and the cell was induced by M-CSF (10 ng/mL) and RANKL (50

142 ng/mL) for further experiment.

143 **Quantitative real-time PCR (qPCR)**

144 After treatment with 50μM of ZA for 48h, total RNA was isolated with Trizol reagent (Sigma-

145 Aldrich) as instructed by the manufacturer. Reverse transcriptional PCR was carried out using the

146 SMART PCR cDNA Synthesis Kits (Clontech). qPCR was carried out on ABI 7500 RealTime

147 PCR System (Applied Biosystem) with powerup SYBR green Mix (ThermoFisher). The fold

148   changes of RNA transcripts were calculated by the $2^{-\Delta\Delta Ct}$ method and the 18s was used as a

149   reference gene. The qPCR primer pairs in Table 1

Western blotting analysis

151   BMDMs-induced osteoclast (1×10^5 cells/well in 12-well plates) were treated with or without

152   ZA(50μM) for 48h, the total protein was isolated using RIPA Buffer (Solarbio, Beijing, China),

153   and total protein concentration was quantified by BCA protein assay kit (Beyotime). 20 μg of

154   protein were separated by 8% SDS-PAGE and transferred to PVDF membranes (Merck Millipore,

155   Billerica, MA, USA). After blocking with 5% bovine serum albumin or 5% nonfat milk, the

156   membranes were incubated with anti-FBXO9 (1:1000, PA5-25475, Thermo Fisher Scientific),

157   p53(1.0 μg/mL, MA5-14067, Thermo Fisher Scientific), ubiquitin (1:2000, ab134953, Abcam),

158   and GAPDH (1:5000, MA1-16757, Thermo Fisher Scientific) overnight at 4 °C. Then the

159   membranes were treated with HRP-conjugated anti-mouse or rabbit secondary antibody (1:5000)

160   for 1h at room temperature.

Co-immunoprecipitation (Co-IP)

162   BMDMs-induced osteoclast were lysed using NP40 buffer (10 mM Tris-HCl at pH 8.0, 140 mM

163   NaCl, 1.5 mM MgCl2, 0.5% Nonidet-P40, 20 mM dithiothreitol, 500 U/mL RNAsin, and 0.5%

164   [w/v] deoxycholate), cell lysates were incubated with FBXO9 (2 μg/ml; PA5-25475) or p53 (2

165   μg/ml; MA5-14067) antibody for 4h, then Protein A/G beads (Thermo Fisher Scientific) were

166   added to the IP reactions and left rotating overnight at 4°C, then beads were washed by PBS

167   containing protein inhibitors for three times, then the immunoprecipitates were analyzed using

168   western blotting with FBXO9 antibody or p53 antibody.

169 **Statistical analysis**

170 All the data are shown as the mean ± standard error of mean (SEM) from three independent

171 experiments. Statistical analysis was carried out using SPSS 19.0 software

172 (IBM Corp., NY. USA). The significance between two groups was analyzed using one-way

173 ANOVA followed by Tukey-Kramer multiple comparisons test or unpaired Student's *t*-test.

174 $p<0.05$ was considered to indicate a statistically significant difference.

175

176 **Results**

177 **ZA treatment facilitated the ferroptosis of osteoclasts**

178 To investigate the function of ZA on osteoclasts, RAW264.7 cells and bone marrow-derived

179 macrophages (BMDMs) were pre-treated with RANKL for 6 days followed by ZA treatment in

180 different concentrations (5, 10, and 50 uM) for 48 hours, the cell model was confirmed byTRAP

181 staining (Figure1 A and B). Cell viability was analyzed by CCK-8 assay. As shown in Figure1 C

182 and D, ZA treatment suppressed cell viability in a dose-dependent manner. The results from FDA

183 staining also showed that the effect of ZA on promoting cell viability of osteoclasts (Figure 1E

184 and F). Impressively, the CCK-8 assay results showed that cell death of osteoclasts induced by ZA

185 treatment was obviously blocked by ferrostatin-1 (Fer-1, a specific inhibitor of ferroptosis) but not

186 necrostatin-1 (a specific inhibitor of necroptosis) and ZVAD-FMK (a specific inhibitor of

187 apoptosis) (Figure 1G and H).

188 To define the role of ZA in the ferroptosis of osteoclasts, the ferroptosis signaling was evaluated

189 in osteoclasts after ZA treatment. As shown in Figure 2A-C and F-H, ZA treatment markedly

190 increased the Fe^{2+} level, MDA content, and ROS level in a dose-dependent manner in osteoclasts,

191 differentiated from RAW264.7 cells and BMDMs, suggesting the promotion of ferroptosis

192 signaling in osteoclasts treated by ZA. Besides, ZA treatment also suppressed the levels of Gpx4

193 and GSH in a dose-dependent manner in osteoclasts (Figure 2D, E, I, and J). These results

194 demonstrate that ZA treatment facilitates the ferroptosis of osteoclasts.

195 **FBXO9 was downregulated in osteoclasts after ZA treatment**

196 To investigate the mechanism underlying ZA-induced osteoclasts ferroptosis, the differentially

197 expressed genes (DEGs) of osteoclasts induced by bisphosphonates alendronate- and risedronate-

198 treatment were obtained from GSE63009, and the common DEGs were identified by venn diagram

199 analysis. As shown in Figure 3A, eighteen common genes were identified (CFAP53, COL14A1,

200 ARSJ, ABCA9, CXorf57, GPR22, STXBP5L, MSANTD4, RRP15, UGT1A2, IRF4, TFAP2D,

201 TRHDE, ASMT, CAPS, COMMD10, VSTM4, FBXO9). The level of these 18 genes was

202 evaluated in osteoclasts treated with or without ZA using qPCR analysis. Figure 3B and C showed

203 that only FBXO9 was significantly decreased in osteoclasts after treatment with ZA. Similar to the

204 qPCR results, the results from western blotting showed that the expression of FBXO9 was

205 obviously decreased in osteoclasts after treatment with ZA. These results indicate that the FBXO9

206 was downregulated by ZA treatment (Figure 3D).

207 **FBXO9 inhibition facilitated the ferroptosis of osteoclasts**

208 To investigate the function of FBXO9 on osteoclasts, the expression of FBXO9 was down-

209 regulated by si-FBXO9 in BMDMs-differentiated osteoclasts. As shown in Figure 4 A-B, the

210 expression of FBXO9 was significantly decreased by si-FBXO9. Cell viability of osteoclasts was

211 significantly decreased in the FBXO9 knockdown group compared with the control group (Figure

212 4C). The results from FDA staining also showed the effect of FBXO9 on inhibiting cell viability

213 (Figure 4D and E).

214   To investigate the role of FBXO9 in ferroptosis of osteoclasts, the ferroptosis signaling was

215 evaluated in osteoclasts differentiated from BMDMs. As shown in Figure 4F-J, FBXO9

216 knockdown significantly increased the Fe^{2+} level, MDA content, ROS level and decreased the

217 GPX4 level, GSH content in osteoclasts. These results suggested that FBXO9 inhibition facilitates

218 the ferroptosis of osteoclasts

219 **ZA treatment facilitated the ferroptosis of osteoclasts by suppressing FBXO9**

220 To explore whether FBXO9 mediated the function of ZA in regulating the ferroptosis of

221 osteoclasts, the osteoclasts differentiated from BMDMs were treated by ZA in the presence or

222 absence of FBXO9. As shown in Figure 5A and B, the qPCR and western blotting analysis results

223 showed that the expressions of FBXO9 were decreased by ZA treatment and restored by FBXO9

224 overexpression. CCK8 results showed that cell viability of osteoclasts was decreased by ZA

225 treatment, but these effects were blocked by FBXO9 overexpression (Figure 5C). Consistently, the

226 FDA staining also showed the inhibition of ZA on osteoclasts cell viability was restored by FBXO9

227 overexpression (Figure 5D and E). Besides, the Fe^{2+} level, MDA content, and ROS level were

228 obviously increased and the GPX4 level, GSH content was significantly decreased by ZA

229 treatment, while these effects were blocked by FBXO9 overexpression (Figure 5F-J). These results

230 suggested that ZA treatment facilitates the ferroptosis of osteoclasts by suppressing FBXO9.

231 **FBXO9 inhibition facilitated the ferroptosis of osteoclasts by blocking the ubiquitin**

232 **mediated-proteasome degradation of p53**

233 Previous studies showed that FBXO9, an E3 ubiquitin ligase, mediated protein stability through

234 ubiquitin mediated-proteasome degradation[20]. Given that dysregulated ubiquitination has been

235 widely reported to be involved in many diseases by regulating cell ferroptosis[26, 27], the target

236 of FBXO9 was predicted by ubibrowser (http://ubibrowser.ncpsb.org.cn/ubibrowser/). Figure 6A

237 showed the 20 potential target genes that interacted with FBXO9. Interestingly, among these

238 genes, the p53 gene is an important regulator of ferroptosis. We next explored whether FBXO9

239 decreases p53 protein level by promoting its ubiquitination-mediated degradation. Knockdown of

240 FBXO9 in osteoclasts did not change the p53 mRNA level (Figure 6B). Fascinatingly, the protein

241 level of p53 was significantly increased after FBXO9 inhibition (Figure 6C), suggesting that

242 FBXO9 decreased p53 expression possibly by the ubiquitin-proteasome-mediated degradation.

243 Next, a reciprocal Co-IP assay was performed to confirm whether FBXO9 directly interacts with

244 p53. As shown in Figure 6D, a positive p53 signal was observed in the protein complex pulled

245 down by FBXO9 antibody. Meanwhile, FBXO9 was also detected in the co-immunoprecipitation

246 complex pulled-down by p53 antibody. Next, cycloheximide assay (CHX) was performed to detect

247 the protein stability of p53 in osteoclasts transfected with si-FBXO9. As shown in Figure 6E, the

248 protein stability of p53 was obviously increased in the FBXO9 knockdown osteoclasts. Then the

249 p53 ubiquitination was assessed through IP with FBXO9 antibody and subsequent western blotting

250 with ubiquitin antibody. Figure 6F showed that FBXO9 knockdown obviously decreased p53

251 ubiquitination in osteoclasts (Figure 6F). in conclusion, these results indicated that FBXO9 directly

252 interacts with p53 and promotes its degradation.

253

Discussion

255 BRONJ is one of the severe complications of BPs administration reported by Marx *et al*. in

256 2003[6]. It usually occurs in patients with bone metastatic cancer or osteoporosis, and undergoes

257 bisphosphonate therapy. ZA is a kind of nitrogen-containing bisphosphonates and is widely used

258 in the treatment of bone metastatic cancer and osteoporosis. Zhu *et al.* reported that ZA facilitates

259 TLR-4-mediated M1 type macrophage polarization in the development of BRONJ[28]. Huang *et*

260 *al.* demonstrated that ZA inhibited osteoclast differentiation and function by regulating the NF-κB

261 and JNK signaling pathways[29]. However, the mechanisms underlying ZA regulates osteoclast

262 function in the occurrence of BRONJ remains unclear. In the current study, we clarified that ZA

263 promotes osteoclasts ferroptosis by inhibiting FBXO9-mediated p53 ubiquitination and

264 degradation, as evidence by (I) ZA treatment facilitated the ferroptosis of osteoclasts; (II) FBXO9

265 was downregulated in osteoclasts after ZA treatment; (III) FBXO9 inhibition facilitated the

266 ferroptosis of osteoclasts; (IV) ZA treatment facilitated the ferroptosis of osteoclasts by

267 suppressing FBXO9;(V) FBXO9 inhibition facilitated the ferroptosis of osteoclasts by blocking

268 the ubiquitin mediated-proteasome degradation of p53.

269 Although a growing body of research have explored the role of BPs in the pathogenesis of

270 BRONJ, the mechanism of BPs on the development of BRONJ is not completely understood.

271 Growing studies have demonstrated that BPs have high affinity to hydroxyapatite crystals, thereby

272 suppressing the osteoclasts resorptive ability by inducing the apoptosis of osteoclasts[30, 31].

273 Moreover, due to the lack of cytokines released by osteoclasts, the differentiation of osteoblasts

274 was blocked, thus suppressing the healing ability of bone, suggesting that the differentiation of

275 osteoclasts plays an important role in the development of BRONJ[32]. More recently, ZA has

276 been reported to inhibit osteoclast differentiation by regulating the NF-κB and JNK signaling

277 pathways[29]. Another study has shown that ZA inhibits osteoclast differentiation by interrupting

278 RANKL/RANK pathway[33]. Consistent with previous studies, we confirmed that ZA decreased

279 cell viability of osteoclasts induced by RANKL, specifically ZA-induced cell viability decrease

280 was blocked by ferroptosis inhibitor, suggesting an important role of ferroptosis in the

281 development of BRONJ.

282   Ferroptosis is a kind of iron- and ROS-dependent form of cell death, different with necrosis,

283 apoptosis, and other forms of cell death. Right now, almost all the mechanisms of ferroptosis are

284 associated with reactive oxygen species (ROS)[12]. Given the role of ZA in regulating ROS

285 production [22-24], here we investigated whether ZA suppresses the growth of osteoclast by

286 accelerating ferroptosis. We found that the ferroptosis-related marker such as the levels of Fe^{2+},

287 MDA content, ROS level was obviously increased in the osteoclasts treated with ZA, suggesting

288 the ZA induced the ferroptosis of osteoclasts. However, the underlying mechanism of ZA-induced

289 osteoclast ferroptosis reminds unknown.

290   To elucidate the mechanism of ZA-induced osteoclast ferroptosis, we compared the

291 expression profiles of osteoclasts in the presence or absence of alendronate or risedronate

292 treatment, and got 18 genes with significant differences in the osteoclasts treated by BPs. Among

293 these18 genes, FBXO9 was identified to be significantly reduced in ZA-treated osteoclasts.

294 Further experiment showed that FBXO9 knockdown promoted the ferroptosis of osteoclasts, and

295   the ferroptosis of osteocalsts induced by ZA was blocked by FBXO9 overexpression, suggesting

296   that ZA promotes the ferroptosis of osteoclasts by downregulating the expression of FBXO9.

297   The F-box only protein 9 (FBXO9), a member of the F-box protein family, is the substrate

298   recognition subunit of skp1-cullin1-f-box E3 ligase complex and plays a key role in ubiquitination

299   and subsequent target protein degradation[19]. Liu *et al.* demonstrated that FBXO9 interacted with

300   Neurog2 and promoted its destabilization is a major contributor in directing multipotent NC

301   progenitors toward glial lineage [20]. Vanesa Fernández-Sáiz *et al.* demonstrated that, under the

302   growth factor deprivation condition, FBXO9-mediated ubiquitination of Tel2 and Tti1 inactivated

303   mTORC1, but activated the PI3K/Akt pathway to increase survival of multiple myeloma[21].

304   However, the function of FBXO9 in the development of BRONJ and the regulatory mechanism

305   remain unclear. Growing studies suggested that E3 ubiquitin ligase regulates ferroptosis by

306   degrading substrates. Yang *et al.* reported that Nedd4 ubiquitylates VDAC2/3 to suppress erastin-

307   induced ferroptosis in melanoma[26]. Another study showed that TRIM26 facilitates the

308   ferroptosis of HSCs to suppress liver fibrosis by mediating the ubiquitination of SLC7A11[35].

309   Therefore, we speculated whether FBXO9 also regulates ferroptosis by mediating the

310   ubiquitination of target genes. Interestingly, we found that p53, a key upstream regulator of

311   ferroptosis, is one of the FBXO9 targets. Our data showed that FBXO9-knowdown did not change

312   the p53 mRNA level but significantly increased the p53 protein level, suggesting that FBXO9-

313   mediated p53 expression by the ubiquitin-proteasome system. Further experiment showed that

314   FBXO9 directly interacts with p53 and the ubiquitination level of p53 was downregulated by

315   FBXO9 knockdown. In addition, the protein stability of p53 was promoted by FBXO9 knockdown.

316 These data suggesting that p53 is the direct target of FBXO9 and FBXO9-mediated p53

317 ubiquitination and degradation in osteoclast.

318 **Conclusions**

319 Taken together, the current data demonstrated that FBXO9 was downregulated in ZA-treated

320 osteoclast and promoted osteoclasts ferroptosis by inhibiting FBXO9-mediated p53 ubiquitination

321 and degradation. Our study provided a possible theoretical target for the clinical treatment of

322 BRONJ.

323 There are still some deficiencies in the current research, such as the current conclusions still need

324 to be further confirmed by clinical and animal experiments.

325 **Conflicts of Interest**

326 The authors declare no competing or financial interests.

327

328 **References**

329 1.   Zhang, S., G. Gangal, and H. Uludag, *'Magic bullets' for bone diseases: progress in rational design of bone-*
330   *seeking medicinal agents.* Chem Soc Rev, 2007. **36**(3): p. 507-31.
331 2.   Black, D.M., et al., *Atypical Femur Fractures: Review of Epidemiology, Relationship to Bisphosphonates,*
332   *Prevention, and Clinical Management.* Endocr Rev, 2019. **40**(2): p. 333-368.
333 3.   La-Beck, N.M., et al., *Repurposing amino-bisphosphonates by liposome formulation for a new role in cancer*
334   *treatment.* Semin Cancer Biol, 2021. **68**: p. 175-185.
335 4.   Favus, M.J., *Bisphosphonates for osteoporosis.* N Engl J Med, 2010. **363**(21): p. 2027-35.
336 5.   Mhaskar, R., et al., *Bisphosphonates in multiple myeloma: an updated network meta-analysis.* Cochrane
337   Database Syst Rev, 2017. **12**: p. CD003188.
338 6.   Marx, R.E., *Pamidronate (Aredia) and zoledronate (Zometa) induced avascular necrosis of the jaws: a*
339   *growing epidemic.* J Oral Maxillofac Surg, 2003. **61**(9): p. 1115-7.
340 7.   Maciel, A.P., et al., *Clinical profile of individuals with bisphosphonate-related osteonecrosis of the jaw: an*
341   *integrative review.* Sao Paulo Med J, 2020. **138**(4): p. 326-335.
342 8.   Hadjidakis, D.J. and Androulakis, II, *Bone remodeling.* Ann N Y Acad Sci, 2006. **1092**: p. 385-96.
343 9.   Ikebuchi, Y., et al., *Coupling of bone resorption and formation by RANKL reverse signalling.* Nature, 2018.

344   **561**(7722): p. 195-200.

345 10. Madel, M.B., et al., *Immune Function and Diversity of Osteoclasts in Normal and Pathological Conditions.*
346   Front Immunol, 2019. **10**: p. 1408.

347 11. Wang, L., et al., *Various pathways of zoledronic acid against osteoclasts and bone cancer metastasis: a brief*
348   *review.* BMC Cancer, 2020. **20**(1): p. 1059.

349 12. Li, J., et al., *Ferroptosis: past, present and future.* Cell Death Dis, 2020. **11**(2): p. 88.

350 13. Hirschhorn, T. and B.R. Stockwell, *The development of the concept of ferroptosis.* Free Radic Biol Med, 2019.
351   **133**: p. 130-143.

352 14. Mou, Y., et al., *Ferroptosis, a new form of cell death: opportunities and challenges in cancer.* J Hematol
353   Oncol, 2019. **12**(1): p. 34.

354 15. Reichert, C.O., et al., *Ferroptosis Mechanisms Involved in Neurodegenerative Diseases.* Int J Mol Sci, 2020.
355   **21**(22).

356 16. Sun, Y., et al., *The emerging role of ferroptosis in inflammation.* Biomed Pharmacother, 2020. **127**: p.
357   110108.

358 17. Bagan, J., et al., *Oxidative stress in bisphosphonate-related osteonecrosis of the jaws.* J Oral Pathol Med,
359   2014. **43**(5): p. 371-7.

360 18. Ma, H., et al., *Melatonin Suppresses Ferroptosis Induced by High Glucose via Activation of the Nrf2/HO-1*
361   *Signaling Pathway in Type 2 Diabetic Osteoporosis.* Oxid Med Cell Longev, 2020. **2020**: p. 9067610.

362 19. Lee, K.W., et al., *F-box only protein 9 is an E3 ubiquitin ligase of PPARgamma.* Exp Mol Med, 2016. **48**: p.
363   e234.

364 20. Liu, J.A., et al., *Fbxo9 functions downstream of Sox10 to determine neuron-glial fate choice in the dorsal root*
365   *ganglia through Neurog2 destabilization.* Proc Natl Acad Sci U S A, 2020. **117**(8): p. 4199-4210.

366 21. Fernandez-Saiz, V., et al., *SCFFbxo9 and CK2 direct the cellular response to growth factor withdrawal via*
367   *Tel2/Tti1 degradation and promote survival in multiple myeloma.* Nat Cell Biol, 2013. **15**(1): p. 72-81.

368 22. Sehitoglu, I., et al., *Zoledronic acid aggravates kidney damage during ischemia reperfusion injury in rat.* J
369   Environ Pathol Toxicol Oncol, 2015. **34**(1): p. 53-61.

370 23. Wang, L., et al., *The apoptotic effect of Zoledronic acid on the nasopharyngeal carcinoma cells via ROS*
371   *mediated chloride channel activation.* Clin Exp Pharmacol Physiol, 2018. **45**(10): p. 1019-1027.

372 24. Liu, L., et al., *Zoledronic Acid Enhanced the Antitumor Effect of Cisplatin on Orthotopic Osteosarcoma by*
373   *ROS-PI3K/AKT Signaling and Attenuated Osteolysis.* Oxid Med Cell Longev, 2021. **2021**: p. 6661534.

374 25. Takahashi, N., et al., *Generating murine osteoclasts from bone marrow.* Methods Mol Med, 2003. **80**: p.
375   129-44.

376 26. Yang, Y., et al., *Nedd4 ubiquitylates VDAC2/3 to suppress erastin-induced ferroptosis in melanoma.* Nat
377   Commun, 2020. **11**(1): p. 433.

378 27. Zhang, Z., et al., *RNA-binding protein ZFP36/TTP protects against ferroptosis by regulating autophagy*
379   *signaling pathway in hepatic stellate cells.* Autophagy, 2020. **16**(8): p. 1482-1505.

380 28. Zhu, W., et al., *Zoledronic acid promotes TLR-4-mediated M1 macrophage polarization in bisphosphonate-*
381   *related osteonecrosis of the jaw.* FASEB J, 2019. **33**(4): p. 5208-5219.

382 29. Huang, X.L., et al., *Zoledronic acid inhibits osteoclast differentiation and function through the regulation of*
383   *NF-kappaB and JNK signalling pathways.* Int J Mol Med, 2019. **44**(2): p. 582-592.

384 30. Favia, G., et al., *Medication-related osteonecrosis of the jaw: Surgical or non-surgical treatment?* Oral Dis,

385   2018. **24**(1-2): p. 238-242.

386 31. Russell, R.G., *Bisphosphonates: the first 40 years.* Bone, 2011. **49**(1): p. 2-19.

387 32. AlDhalaan, N.A., A. BaQais, and A. Al-Omar, *Medication-related Osteonecrosis of the Jaw: A Review.* Cureus,

388   2020. **12**(2): p. e6944.

389 33. Li, M., et al., *Regulation of osteogenesis and osteoclastogenesis by zoledronic acid loaded on biodegradable*

390   *magnesium-strontium alloy.* Sci Rep, 2019. **9**(1): p. 933.

391 34. Tamaoka, J., et al., *Osteonecrosis of the jaws caused by bisphosphonate treatment and oxidative stress in*

392   *mice.* Exp Ther Med, 2019. **17**(2): p. 1440-1448.

393 35. Zhu, Y., et al., *TRIM26 Induces Ferroptosis to Inhibit Hepatic Stellate Cell Activation and Mitigate Liver*

394   *Fibrosis Through Mediating SLC7A11 Ubiquitination.* Front Cell Dev Biol, 2021. **9**: p. 644901.

395

396   **Figure legends**

397   **Figure 1.ZA treatment facilitated the ferroptosis of osteoclasts**

398   The osteoclasts cell model induced by RANKL (50 ng/ml) treatment. (A and B) Multinucleated

399   cells were visualized by tartrate-resistant acid phosphatase (TRAP) staining.(C and D) Cell

400   viability of Raw264.7 and BMDM derived osteoclasts was assessed using CCK8 assay after

401   treatment with different concentrations of ZA (5,10, and 50 μM) (n = 3). (E and F) Cell viability

402   of Raw264.7 and BMDM derived osteoclasts was assessed using FDA staining after treatment

403   with different concentrations of ZA (5,10, and 50 μM) (n = 3). (G and H) Cell viability of

404   Raw264.7 and BMDM derived osteoclasts was assessed using CCK8 assay after treatment with

405   ZA for 48h (50 μM) in the presence or absence of 10μM of ZVAD-FMK, 2μM of Fer-1, or 10μM

406   of necrostatin-1(n = 3). *$p<0.05$, **$p<0.01$.

407   **Figure 2. ZA treatment facilitated the ferroptosis of osteoclasts**

408   (A-E) the level of Fe^{2+}, MDA content, ROS level, the level of Gpx4, and GSH content in Raw264.7

409   derived osteoclasts was assessed by Elisa assay after treatment with different concentrations of ZA

410   (5,10, and 50 μM) (n=3) *$p<0.05$, **$p<0.01$, ***$p<0.001$. (F-J) the level of Fe^{2+}, MDA content,

411   ROS level, the level of Gpx4, and GSH content in BMDM derived osteoclasts was assessed by

412   Elisa assay after treatment with different concentrations of ZA (5,10, and 50 μM) (n=3) *$p<0.05$,

413   **$p<0.01$, ***$p<0.001$.

414   **Figure 3. FBXO9 was downregulated in osteoclasts after ZA treatment**

415   (A) Venn analysis of DEGs of alendronate and risedronate-treated osteoclast. (B and C) The

416   mRNA level of 18 genes in Raw264.7 and BMDM derived osteoclasts was assessed using qPCR

417   after treatment with ZA (50 μM) (n=3) *$p<0.05$, **$p<0.01$. (D) The protein level of FBXO9 in

418   Raw264.7 and BMDM derived osteoclasts was assessed using western blot after treatment with

419   ZA (50 μM)

420   **Figure 4. FBXO9 inhibition facilitated the ferroptosis of osteoclasts**

421   (A) The mRNA level of FBXO9 in BMDM derived osteoclasts was assessed using qPCR after

422   treatment with or without si-FBXO9 (n=3). ***$p<0.001$. (B) The protein level of FBXO9 in

423   BMDM derived osteoclasts was assessed using western blot after treatment with or without si-

424   FBXO9 (n=3). **$p<0.01$. (C)Cell viability of BMDM derived osteoclasts was assessed using

425   CCK8 assay after treatment with or without si-FBXO9 (n=3). **$p<0.01$. (D and E) Cell viability

426   of BMDM derived osteoclasts was assessed using FDA staining after treatment with or without si-

427   FBXO9 (n=3). *$p<0.05$. (F-J) the level of Fe^{2+}, MDA content, ROS level, the level of Gpx4, and

428   GSH content in BMDM derived osteoclasts was assessed by Elisa assay after treatment with or

429   without si-FBXO9 (n = 3) *$p<0.05$, **$p<0.01$.

430   **Figure 5. ZA treatment facilitated the ferroptosis of osteoclasts by suppressing FBXO9**

431   (A) The mRNA level of FBXO9 in BMDM derived osteoclasts was assessed using qPCR after

432   treatment with ZA (50 μM) in the presence or absence of FBXO9 (n=3). **$p<0.01$. (B) The protein

433   level of FBXO9 in BMDM derived osteoclasts was assessed using western blot after treatment

434   with ZA (50 μM) in the presence or absence of FBXO9 (n=3). *$p<0.05$. (C) Cell viability of

435   BMDM derived osteoclasts was assessed using CCK8 assay after treatment with ZA (50 μM) in

436   the presence or absence of FBXO9 (n=3). *$p<0.05$, **$p<0.01$. (D and E) Cell viability of BMDM

437   derived osteoclasts was assessed using FDA staining after treatment with ZA (50 μM) in the

438   presence or absence of FBXO9 (n=3). *$p<0.05$. (F-J) the level of Fe^{2+}, MDA content, ROS level,

439   the level of Gpx4, and GSH content in BMDM derived osteoclasts was assessed by Elisa assay

440   after treatment with ZA (50 μM) in the presence or absence of FBXO9 (n = 3) *$p<0.05$, **$p<0.01$.

441   **Figure 6. FBXO9 inhibition facilitated the ferroptosis of osteoclasts by blocking the ubiquitin**

442   **mediated-proteasome degradation of p53**

443   (A) The target of FBXO9 was predicted by ubibrowser. (B) the p53 mRNA expression in the

444   FBXO9 knockdown and control cell was assessed by qPCR (n=3). (C) the protein level of p53 in

445   the FBXO9 knockdown and control cell was assessed by western blot (n=3). (D) FBXO9 directly

446   interacts with p53. The proteins from BMDM derived osteoclasts were IP with IgG or antibodies

447   against FBXO9 and p53, following by western blot analysis (n=3). (E) The stability of p53 protein

448   was regulated by FBXO9. BMDM derived osteoclasts treated with or without si-FBXO9 in the

449   presence of cycloheximide (CHX, 25 ug/ml) for various times as indicated and cell lysates were

450   then assessed by western blot (n=3). **$p<0.01$. (F) The cell lysates isolated from scramble and si-

451   FBXO9 infected BMDM derived osteoclasts were immunoprecipitated with anti-p53 antibody,

452   then analyzed by western blot using ubiquitin antibody (n=3).

sequence

sequence

1   CFAP53:

2   forward primer:5'-GACAAAATGAGAGAGAGAACCAAGT-3'

3   reverse primer: 5'-TCCCTGAACTGCTGGTCTAAC-3'

4   COL14A1

5   forward primer:5′-ACTGGTTTTCACGGGTGTTC-3′,

6   reverse primer: 5′-TAAGTCGAGGAGAGGCAAGC-3′

7   ARSJ

8   forward primer:5′- CTGAGATAAAGACGCCCACC-3′,

9   reverse primer: 5′- ATAGAATGCTGAAGTCCCGTG-3′

10   ABCA9

11   forward primer:5′- CAGAGGGAGTGAAGAGAAAGC -3′,

12   reverse primer: 5′- GCTCTGTGTTTGTGAAAGTGG -3′

13   CXorf57:

14   forward primer:5′- GCAGTATAGGGAACAAAAGCG-3′,

15   reverse primer: 5′- TGCTTGAGATGTTGAGGGAC-3′

16   GPR22:

17   forward primer:5′- CCACTGTCATACCCACTAAGC-3′,

18   reverse primer: 5′- ATGCAGTAAAGTACCAGGACG-3′

19   STXBP5L:

20   forward primer:5′- GATCAAGTGACCTGTACCAGC-3′,

21   reverse primer: 5′- ATTTACATGGTCTGAGGTGGG-3′

22   MSANTD4

23   forward primer:5′- CAGAGGTCAAAGTGGAAGAGG-3′,

24   reverse primer: 5′- ATCAATGTGAGGGAAGTCAGG-3′

25   RRP15

26   forward primer:5′- GAAATGCTGTGCAGAGTGAAG-3′,

27   reverse primer: 5′- TCCTGCTTCCTTAACCTTTTCG-3′

28   UGT1A2

29   forward primer:5′- TCTGCGTTCTCTTTCCTGTG -3′,

30   reverse primer: 5′- AGCATGTTCTGGACCCTTTG -3′

31   IRF4

32   forward primer:5′- AACAAGCTAGAAAGAGACCAGAC-3′,

33   reverse primer: 5′- TCACCAAAGCACAGAGTCAC-3′

34   TFAP2D

35   forward primer:5′- AAAGATGATCCTAGCCACCAAG-3′,

36   reverse primer: 5′- TGTGTTAAGTGCCTCTGGATG-3′

37   TRHDE

38   forward primer:5′- AGGAAGGCTTTGCTCACTAC -3′,

39   reverse primer: 5′- CTGTGATACTGGATGGGAACTG -3′

40   ASMT

41   forward primer:5′- GAAGTGGGACAGGAAGTGAG -3′,

42   reverse primer: 5′- CGGGAACAGGAAGTGGC -3′

43   CAPS

44   forward primer:5′- AGCTCGAAGACACAATCCG -3′,

45   reverse primer: 5′- TCCATGTCCACTGCAAAGAG -3′

46   COMMD10

47   forward primer:5′- AGTGGGATGGCAGCTTAAC-3′,

48   reverse primer: 5′- TCGAACAGCTCCTTGTGATTG-3′

49   VSTM4

50   forward primer:5′- CCTGGCAGTCTGTGTTTCA-3′,

51   reverse primer: 5′- CTCTTACCCTTCTGTGGCTG-3′

52   FBXO9

53   forward primer:5′- ATGAGAGTCCGGCTGAGAGA-3′,

54   reverse primer: 5′- AGAGCTTCTTCCTGCTCTGC-3′

55   18s

56   forward primer:5′- CTCAACACGGGAAACCTCAC-3′,

57   reverse primer: 5′- CGCTCCACCAACTAAGAACG-3′

Figure 1

ZA treatment facilitated the ferroptosis of osteoclasts

ZA treatment facilitated the ferroptosis of osteoclasts

A

RAW264.7+RANKL

Control   ZOL 5 μM   ZOL 10 μM   ZOL 50 μM

B

BMDM+RANKL

Control   ZOL 5 μM   ZOL 10 μM   ZOL 50 μM

C

Raw264.7+RANKL

D

BMDM+RANKL

E

FDA staining

Control   ZOL (5 μ M)

ZOL (10 μ M)   ZOL (50 μ M)

Raw264.7+RANKL

F

FDA staining

Control   ZOL (5 μ M)

ZOL (10 μ M)   ZOL (50 μ M)

BMDM+RANKL

G

Raw264.7+RANKL

Control
necrostatin-1
ZVAD-FMK
Ferrostatin-1

H

BMDM+RANKL

Control
necrostatin-1
ZVAD-FMK
Ferrostatin-1
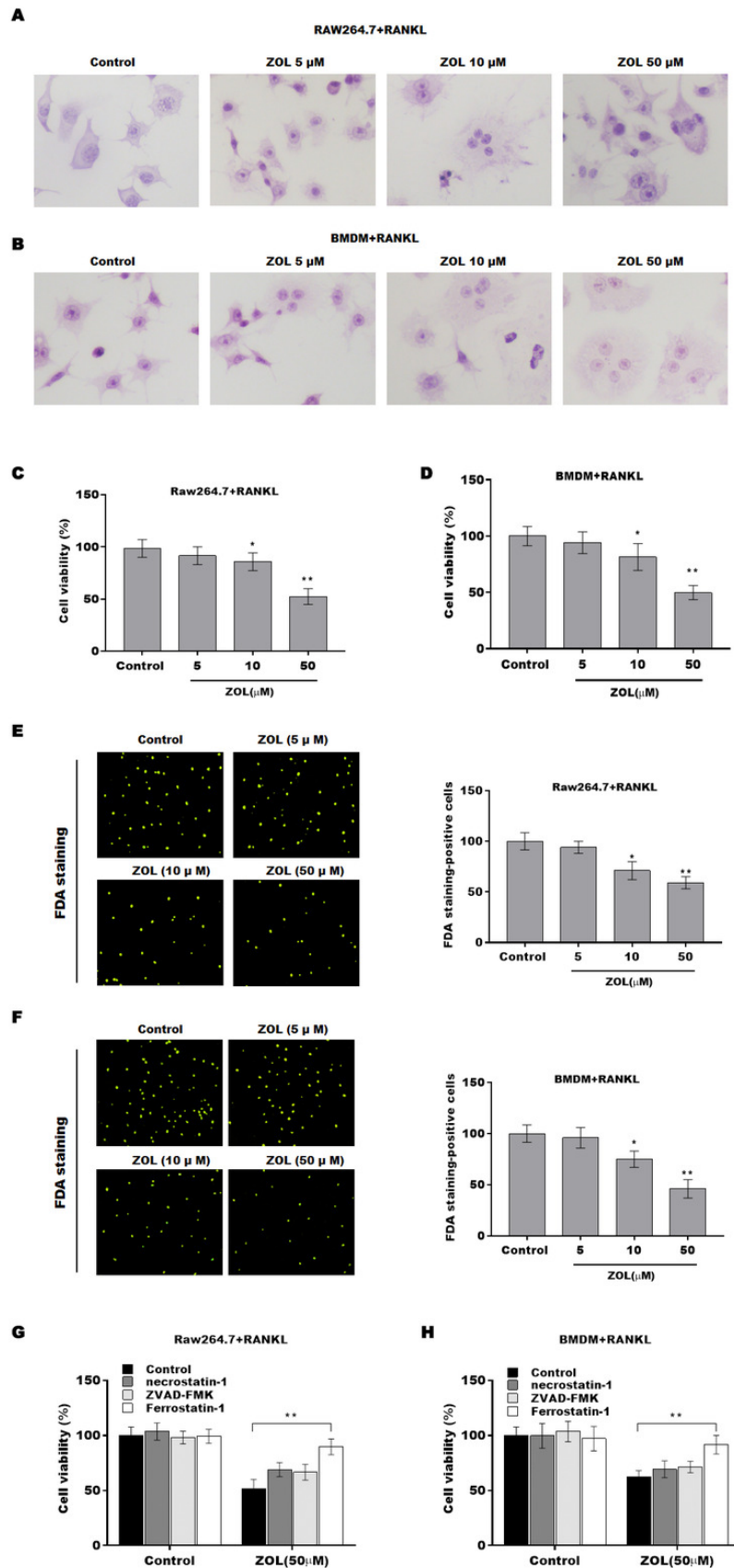
Figure 2

ZA treatment facilitated the ferroptosis of osteoclasts

ZA treatment facilitated the ferroptosis of osteoclasts
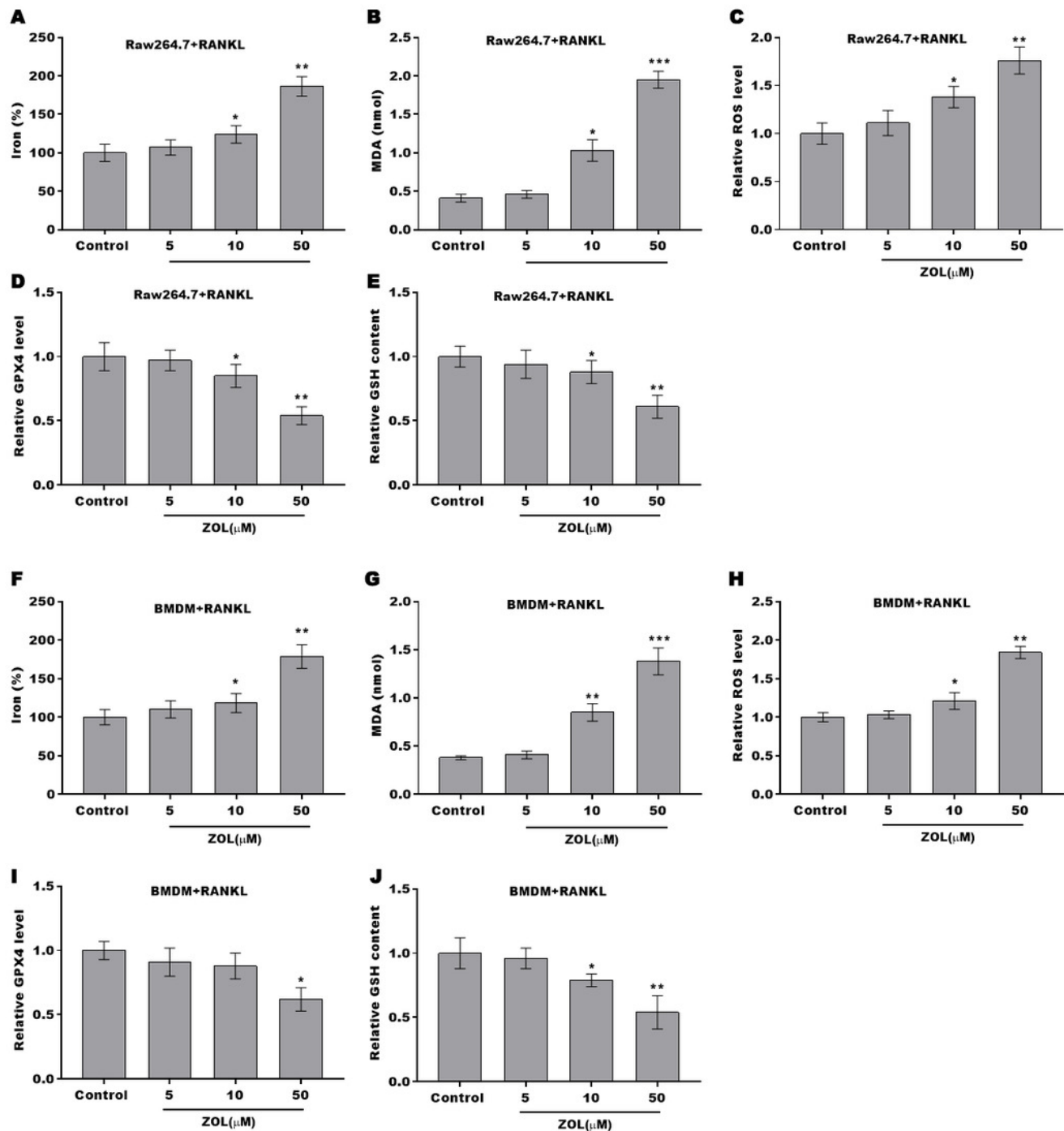
Figure 3

FBXO9 was downregulated in osteoclasts after ZA treatment

FBXO9 was downregulated in osteoclasts after ZA treatment
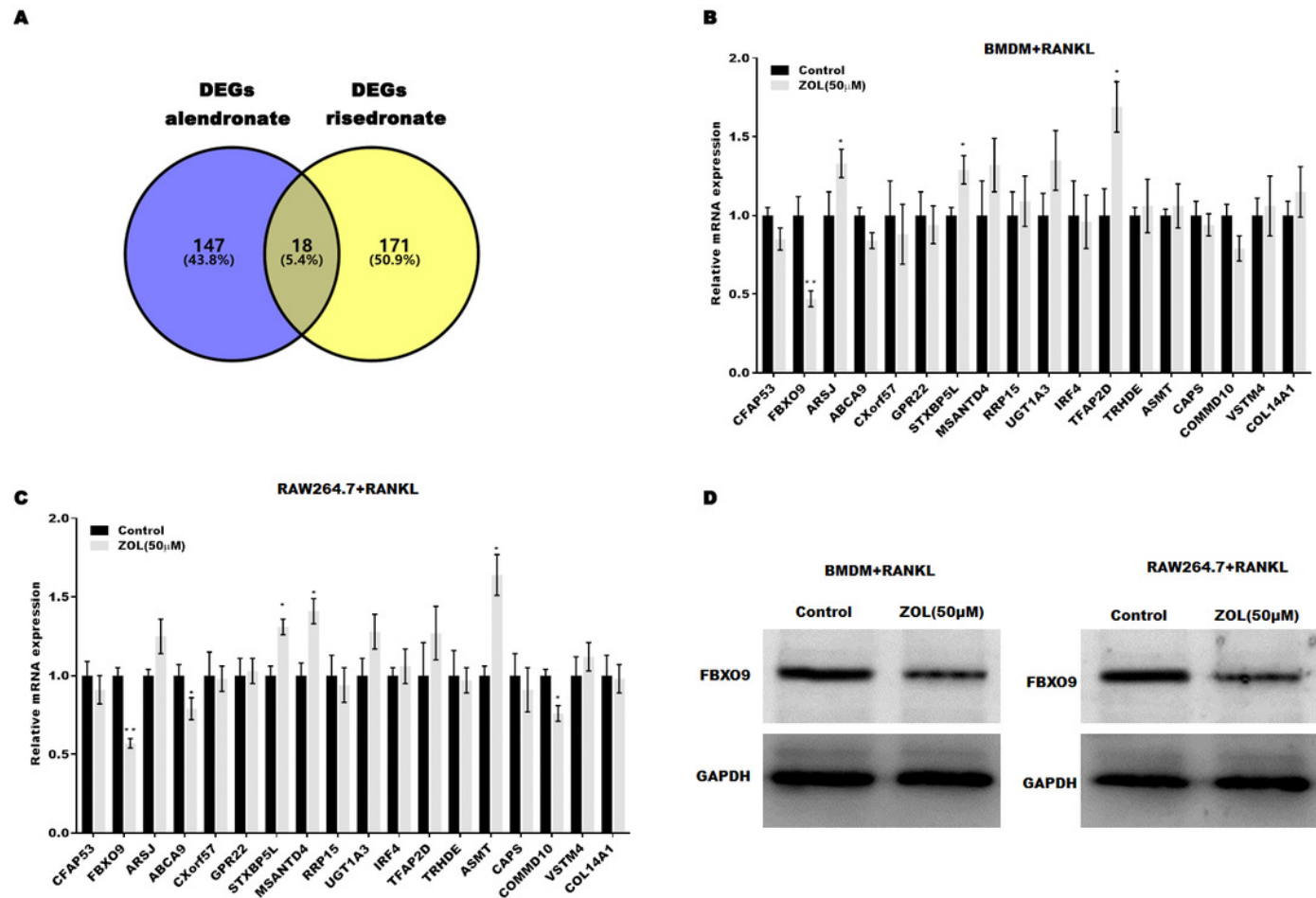
Figure 4

FBXO9 inhibition facilitated the ferroptosis of osteoclasts

FBXO9 inhibition facilitated the ferroptosis of osteoclasts
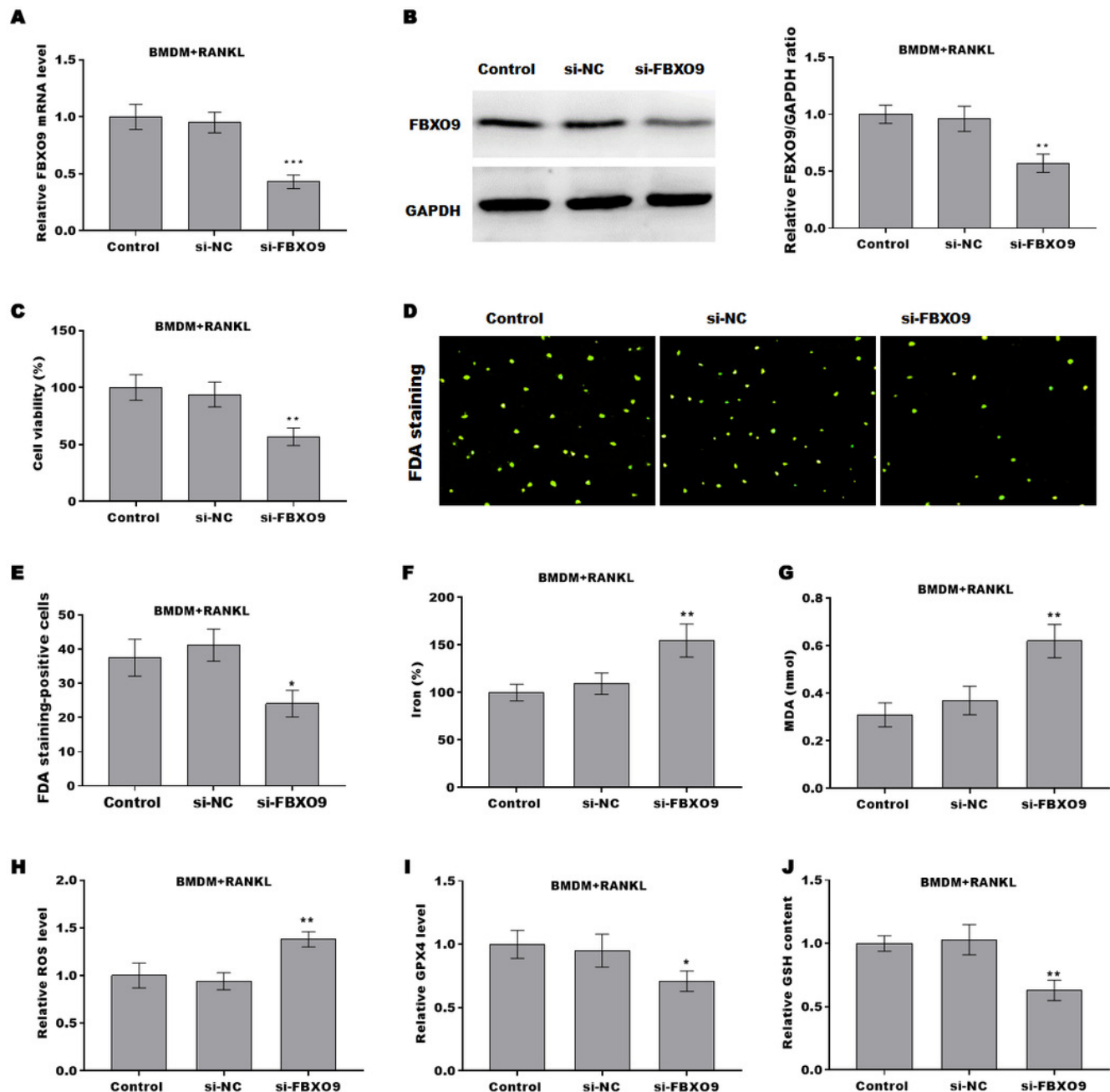
Figure 5

ZA treatment facilitated the ferroptosis of osteoclasts by suppressing FBXO9

ZA treatment facilitated the ferroptosis of osteoclasts by suppressing FBXO9

Figure 6

FBXO9 inhibition facilitated the ferroptosis of osteoclasts by blocking the ubiquitin mediated-proteasome degradation of p53

FBXO9 inhibition facilitated the ferroptosis of osteoclasts by blocking the ubiquitin mediated-proteasome degradation of p53